

Mapping Seismic Hazard in the Central and Eastern United States

Arthur Frankel

U.S. Geological Survey
Denver

INTRODUCTION

The U.S. Geological Survey (USGS) has been publishing probabilistic seismic hazard maps for the United States since 1976 (e.g., Algermissen and Perkins, 1976; Algermissen *et al.*, 1990). We are preparing new national maps for the 1997 edition of the *NEHRP Recommended Provisions for the Development of Seismic Regulations for New Buildings*, published by the Building Seismic Safety Council (NEHRP stands for National Earthquake Hazards Reduction Program). The USGS hazard maps are to be the basis for design value maps for buildings to be included in the *Provisions*. We are conducting a series of regional workshops to discuss the methodology and input to the maps. As of this writing, workshops have been held in the Pacific Northwest, the northeastern U.S., and northern California. We intend to make maps showing ground motions with 10% probability of exceedance (PE) in 50, 100, and 250 years. These correspond to return times of 475, 950, and 2,373 years, respectively. These maps will depict peak ground acceleration and response spectral values at various periods.

This paper is a progress report on the mapping effort for the central and eastern U.S. I describe the basic methodology for hazard mapping in this region that was presented at the northeast workshop and endorsed by most of the workshop participants for maps with return times of 1000 years and less (annual PE's of 10^{-3} and larger). This methodology uses four models to characterize hazard. These models are based on historical seismicity that has been spatially-smoothed to different length scales. This differs from the traditional approach where area source zones are drawn around seismicity or tectonic provinces for the calculation of seismic hazard (see Cornell, 1968).

In this paper, I present trial seismic hazard maps based on this methodology. These maps are for illustrative purposes only and they are not intended to be used in any application.

Some previous studies have also used smoothed versions of the historical seismicity (the "pseudo-historic method") to make hazard calculations, although with significant differences from our approach. Veneziano and Pais (1986) developed a method of automatically assigning source zones from a seismicity catalog. T. F. O'Hara (unpub-

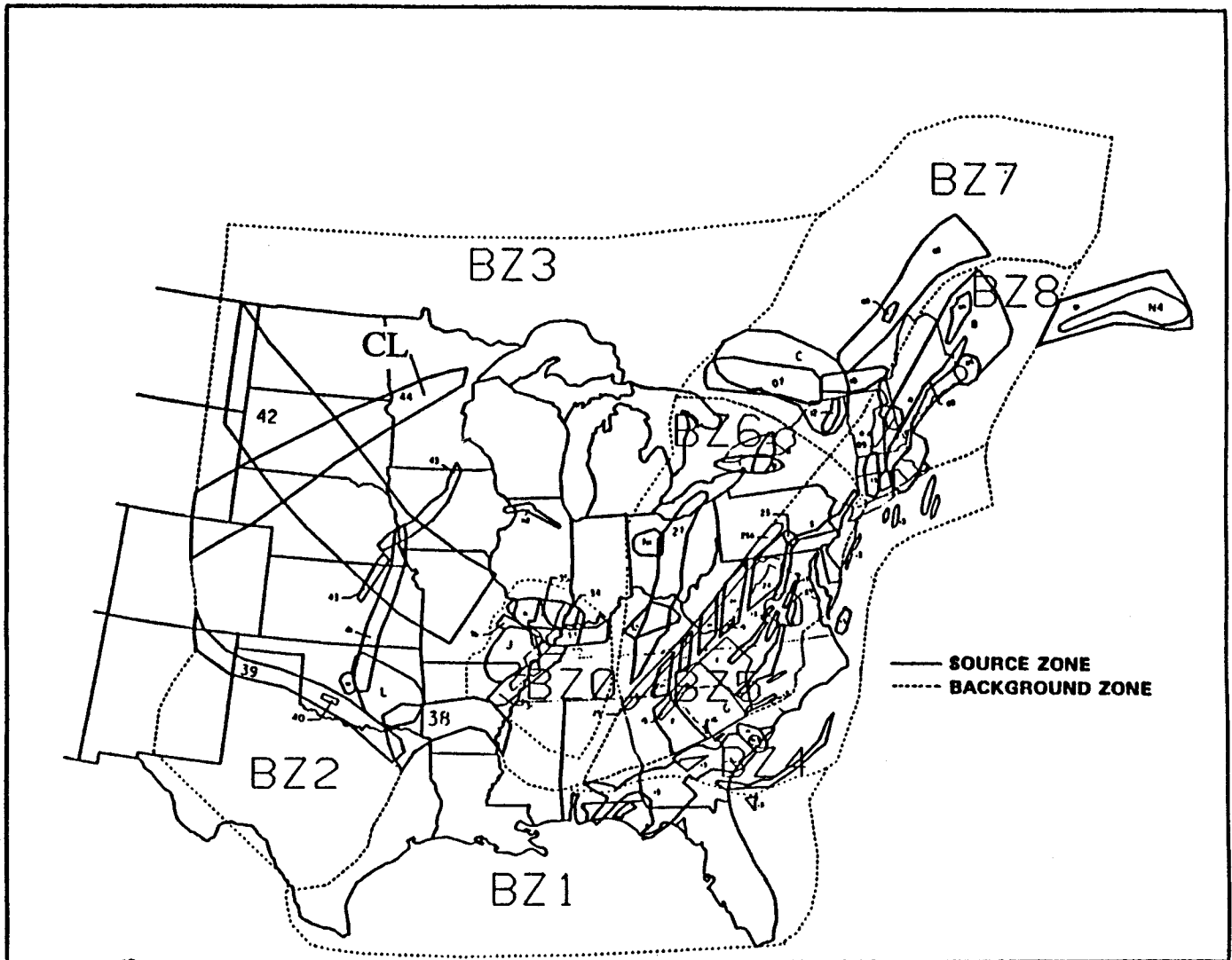
lished report) made hazard calculations at specific sites based on seismicity parameters determined in 1 degree bins from historical seismicity. D. M. Perkins (pers. comm.) made hazard maps by spreading out the locations of past earthquakes. The most similar approach to ours was presented in Jacob *et al.* (1994), who produced hazard maps for the New York State region by spatially smoothing activity rates derived from $M \geq 2$ earthquakes from a local seismic network and $M \geq 3.5$ from the catalog of Seeber and Armbruster (1991).

One of the motivations for directly using the smoothed historical seismicity is to get away from the judgments involved in drawing seismic source zones in a region where the causative structures of seismicity are largely unknown, such as the central and eastern U.S. In some respects, our approach goes against a recent trend in seismic hazard analysis for using several experts to choose separate sets of source zones. The hazard curves determined from these source zone models are then used to calculate mean and median hazard curves, along with a measure of the uncertainty. Recent examples of this type of effort are the studies conducted by the Electric Power Research Institute (EPRI, 1986) and Lawrence Livermore National Laboratory (LLNL; Bernreuter *et al.*, 1989) to assess hazard at nuclear power plant sites in the central and eastern U.S.

I compare the results of our method with those from the EPRI study, where six teams of experts determined sets of area source zones. Figure 1 shows the source zones chosen by one of the expert teams (Bechtel) for the EPRI study. The source zone maps of the other teams have similar complexity. These source zones are based on an assessment of the activity of possible tectonic features using seismic, geophysical, and geological information. I will show that the simple methodology described in this paper produces similar values of mean probability of exceedance as the more involved EPRI study.

METHOD

Figure 2 diagrams the four-model method used in this paper. Maps based on these models will be described later in the paper. First, I consider the hazard from earthquakes with moment magnitudes M less than or equal to 7.0. I use a minimum m_b of 4.5 for the hazard calculation, based on the



▲ **Figure 1** Source zones chosen by the Bechtel team for the EPRI study. Figure taken from EPRI (1986), used by permission of EPRI. "CL" indicates Colorado Lineament source zone.

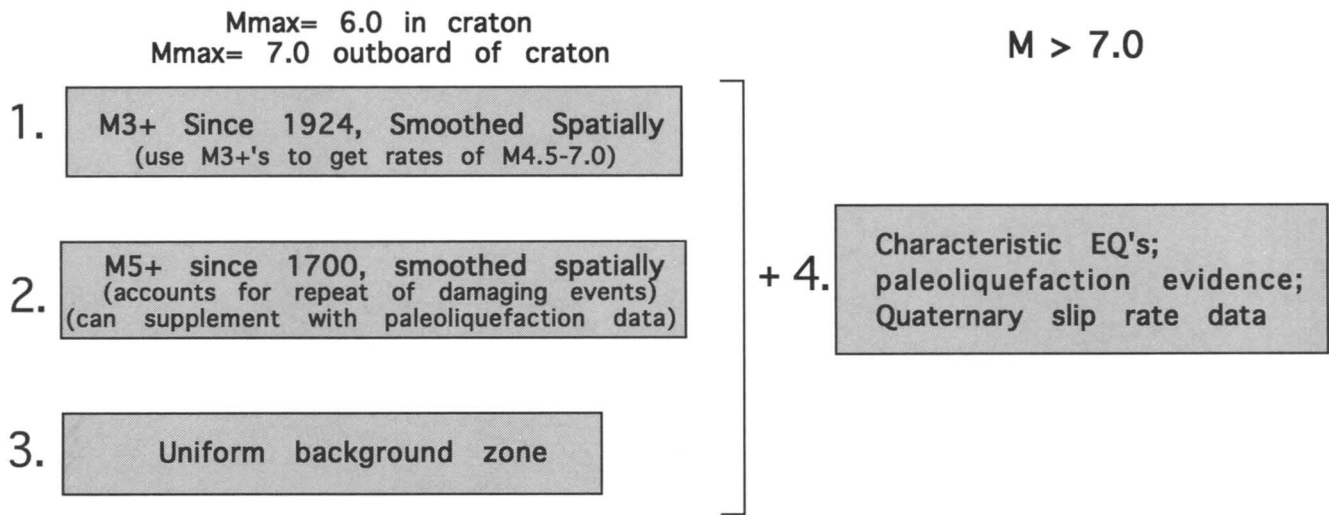
observation that earthquakes less than magnitude 4.5 do not usually cause damage to structures in the eastern U.S. Three alternative models of hazard are used for this magnitude range (Figure 2 left). Model 1 is based on spatially-smoothed a -values derived from the magnitude 3 and larger earthquakes since 1924. Here a is the activity level in the Gutenberg-Richter equation $\log N = a - bM$, where N is the number of events with magnitudes greater or equal to M . In this model, the magnitude 3 and greater events are assumed to illuminate areas of faulting which can produce destructive events. This assumption will be examined further in a later section of the paper.

I use the catalog of eastern North American earthquakes up to 1984 compiled by Seeber and Armbruster (1991). They started with the catalog derived by EPRI and revised some of the magnitudes of historical earthquakes using felt areas rather than maximum intensities, based on the felt area- m_b relations of Sibol *et al.* (1987). To assess catalog complete-

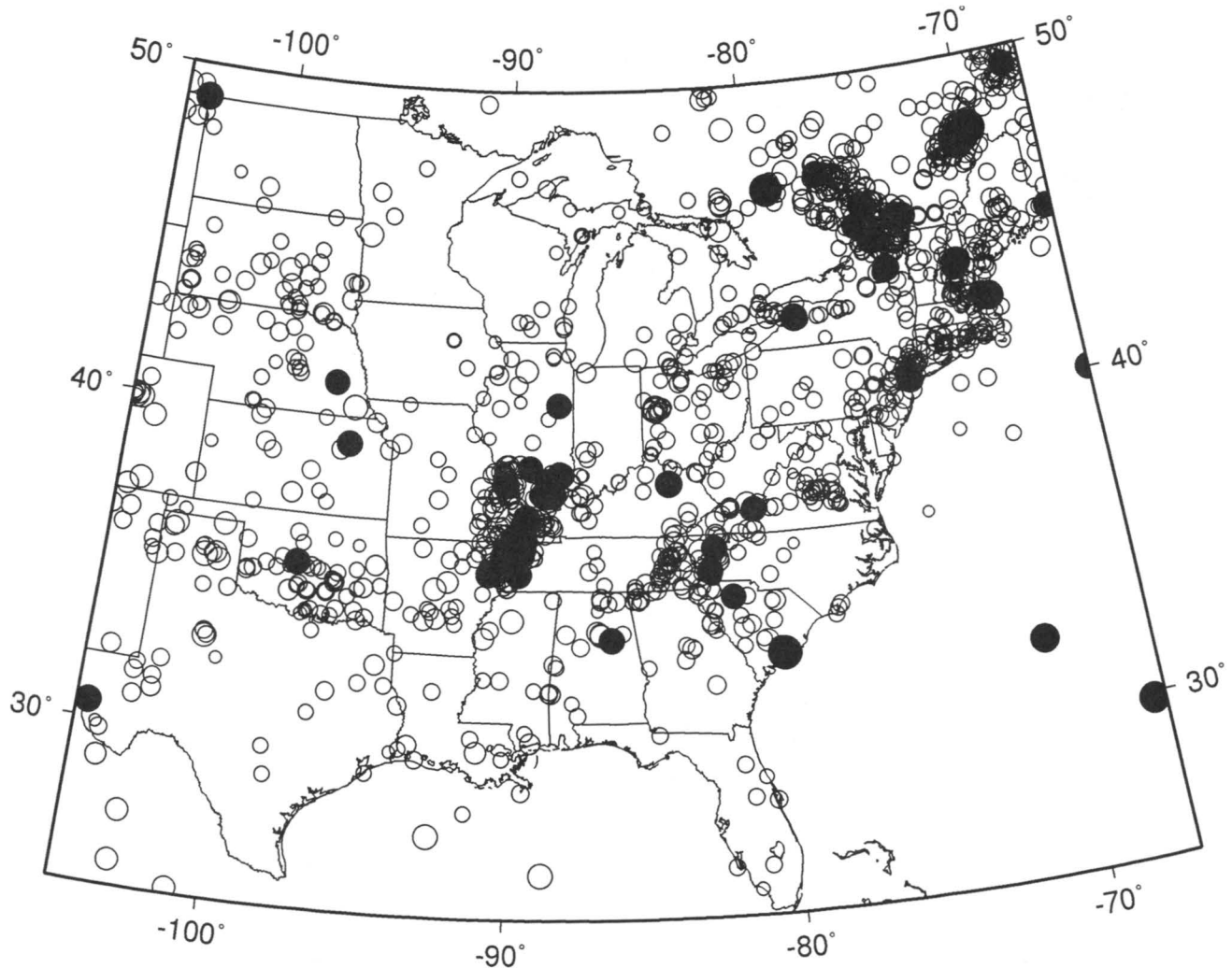
ness, I made plots of cumulative number of events against time for different regions. When events with magnitudes between 3.0 and 3.5 are used, these plots are approximately linear for times after 1924. I therefore assume that the catalog is roughly complete down to magnitude 3.0 since 1924. Figure 3 shows m_b 3 and larger events since 1924 from the Seeber and Armbruster (1991) catalog after foreshocks and aftershocks were removed from the catalog by M. G. Hopper, using a procedure based on the spatial and temporal clustering of events. The calculations in this paper were based on this mainshock catalog.

Figure 3 also displays locations of earthquakes with m_b 5.0 and larger since 1700, from Seeber and Armbruster (1991). For the most part, these earthquakes occurred at or near where there are concentrations of magnitude 3 earthquakes since 1924. Examples of this include the New Madrid, Charlevoix, Ottawa-Cornwall, Attica, central New Hampshire, western North Carolina, and central Oklahoma areas.

Alternative Models of Seismic Hazard For Central and Eastern U.S.



▲ **Figure 2** Chart of four models used in this paper to make seismic hazard maps in the central and eastern U.S.



▲ **Figure 3** Map showing $3.0 \leq mb \leq 4.9$ events (open circles) since 1924 from the Seeber and Armbruster (1991) catalog (aftershocks removed). Size of circles proportional to magnitude. $mb \geq 5.0$ events since 1700 are shown as filled circles.

In the latter five cases, there were substantial numbers of magnitude 3–4 events before the occurrence of the magnitude 5 and larger ones in each area. Of course, New Madrid and Charlevoix have an extensive history of large earthquakes. The area of the m_b 6.2 Timiskaming, Quebec earthquake of 1935 did not previously have magnitude 3 events reported, but this may be due to catalog incompleteness for this sparsely-populated region. It is not known whether the m_b 5 earthquakes in the 1800's in eastern Nebraska and Kansas occurred near previous m_b 3 earthquakes. Since 1924, there have been a few m_b 3 earthquakes in the vicinity. There were some earlier m_b 3 events in the vicinity of the 1980 Sharpsburg, Kentucky (m_b 5.2) earthquake.

For the hazard maps we are making, we are attempting to assess the relative likelihood of moderate earthquakes ($m_b > 5$) for about the next 50–100 years. Looking over the past 60 years, we see that moderate earthquakes generally occur in areas where there have been significant numbers of magnitude 3 events. Therefore, these magnitude 3 events are a reasonable guide to where moderate earthquakes will most likely occur over the next 50 years. This is the motivation for model 1. Models 2 and 3 represent alternative approaches to hazard assessment.

Model 2 uses spatially-smoothed a -values based on the magnitude 5 and above events since 1700. This model assumes that future $m_b \geq 5.0$ events will occur near where they have occurred in the past. This model is intended to account for the possibility of very localized seismogenic structures which repeatedly generate moderate ($m_b \geq 5.0$) earthquakes. It also addresses the observation that magnitude 5 and larger events have occasionally occurred in areas which exhibit few magnitude 3 events since 1924, such as eastern Nebraska and Kansas. Obviously, the historic record is not complete for earthquakes of magnitude 5 and greater since 1700. In that sense, this model will be incomplete. However, model 2 assigns higher hazard in areas that have had moderate or large (magnitude 5 and larger) earthquakes in the past. Since we don't know with certainty the cause of major earthquakes in the central and eastern U.S., it is prudent to address the possibility of near-repeats of historic moderate earthquakes. By "near-repeat", I refer to the possible occurrence of a future moderate earthquake within about 100 km of an historic moderate earthquake. Model 2 also ensures that the hazard map reflects the local, historic rate of magnitude 5 and larger events.

Model 3 takes the opposite approach from model 2. This model is based on a uniform source zone encompassing the entire central and eastern United States. This model was suggested by participants of the northeast workshop. This model covers the possibility of having a moderate earthquake (m_b 5–7.0) in areas that have been quiescent historically. In essence, this model smooths the observed seismicity over the entire region.

Most participants of the northeast workshop agreed that the maximum magnitude (M_{max}) should be differentiated between the craton and areas outboard of the craton. The

workshop attendees suggested a maximum magnitude of 6.0 for the craton and 7.0 for outside the craton, on a trial basis. These values may be altered after input from subsequent workshops.

Each of the three models is constrained to preserve the historic rate of magnitude 5 and larger earthquakes observed since 1924. For model 2, the rate of m_b 5 and larger earthquakes since 1700 is less than that since 1924, probably because of incompleteness of the early portions of the catalog. In the hazard calculation for model 2, I multiplied the rate of occurrence of m_b 5 and larger earthquakes by a factor of 1.39, which is the ratio of the rate of m_b 5 and larger earthquakes since 1924 to that since 1700.

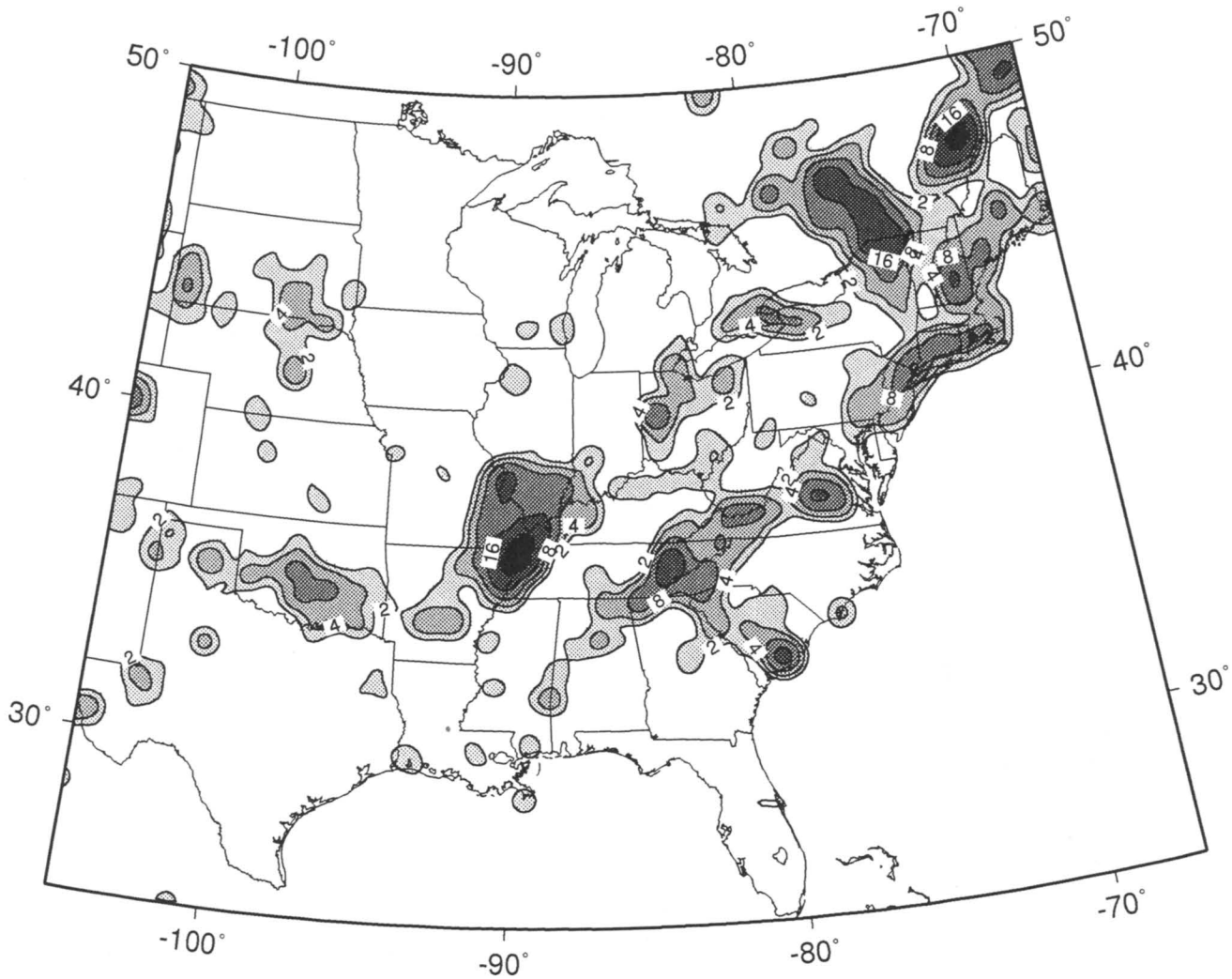
The three models can be used to make uncertainty calculations. They represent a gamut of models, from assuming that events with magnitudes between 5.0 and M_{max} will occur near where they occurred historically (model 2) to assuming that these events can occur anywhere with equal likelihood (model 3). Model 1 represents an intermediate case. These models consider seismic hazard with different scale lengths.

The hazard from large events with moment magnitudes greater than 7.0 must also be added (Figure 2 right; model 4). These events are thought to be limited to a few areas in the central and eastern U.S., such as New Madrid, Wabash Valley, near Charleston, South Carolina, and the Meers Fault in Oklahoma. Future work on paleoliquefaction may identify other areas in the central and eastern U.S. that can generate these large events. I assume that these large events occur as characteristic earthquake, that is, earthquakes having a narrow magnitude range, rather than using a broad range in magnitudes based on the Gutenberg-Richter recurrence relation. The magnitude can be constrained by isoseismal areas for historical events (e.g., Johnston, 1995) or by the areal extent of paleoliquefaction features for pre-historic earthquakes (e.g., Obermeier *et al.*, 1992). Again, this procedure may be modified after input from subsequent workshops.

To make a single probabilistic hazard map, the probabilities of exceedance (see below) from models 1–3 are added together after each model is multiplied by a weight. These weights add to one so that the final model will preserve the historic rate of magnitude 5 and larger earthquakes. Then the probabilities from model 4 are added. This model will have a weight of one, since it is the only model which considers earthquakes with magnitudes greater than 7.0. Alternatively, a hazard map can be produced showing the worst case of the three models with model 4 added to each..

HAZARD CALCULATION

Models 1 and 2 are based on spatially-smoothed historical seismicity. First I count the number of earthquakes n_i with magnitude greater than M_{ref} in each cell i of a grid with spacing of 0.1° in latitude and 0.12° in longitude (about 11 km on a side). This count represents the maximum likelihood estimate of 10^a for that cell (see Weichert, 1980;



▲ **Figure 4** Contour map of smoothed 10^3 values derived from m_b 3 and larger earthquakes since 1924 (correlation distance of 50 km). The values represent number of events in 11 km square grid cell, for 60 years, with magnitude between 0 and 0.1.

Bender, 1983), for earthquakes above M_{ref} . The values of n_i are converted from cumulative values (*i.e.*, number of events above M_{ref}) to incremental values (*i.e.*, number of events from M_{ref} to $M_{ref} + \Delta M$) using the formula of Herrmann (1977).

The grid of n_i values is then smoothed spatially by multiplying by a Gaussian function with correlation distance c . For each cell i , the smoothed value \tilde{n}_i is obtained from

$$\tilde{n}_i = \frac{\sum_j n_j e^{-\Delta_{ij}^2/c^2}}{\sum_j e^{-\Delta_{ij}^2/c^2}} \quad (1)$$

In this equation, \tilde{n}_i is normalized to preserve the total number of events. Δ_{ij} is the distance between the i th and j th cells. The sum is taken over cells j within a distance of $3c$ of cell i .

The annual probability of exceeding specified ground motions is calculated for a grid of sites using \tilde{n}_i from equation (1). For each site, the values of \tilde{n}_i are binned by their distance

from that site, so that N_k denotes the total of \tilde{n}_i values for cells within a certain distance increment of the site.

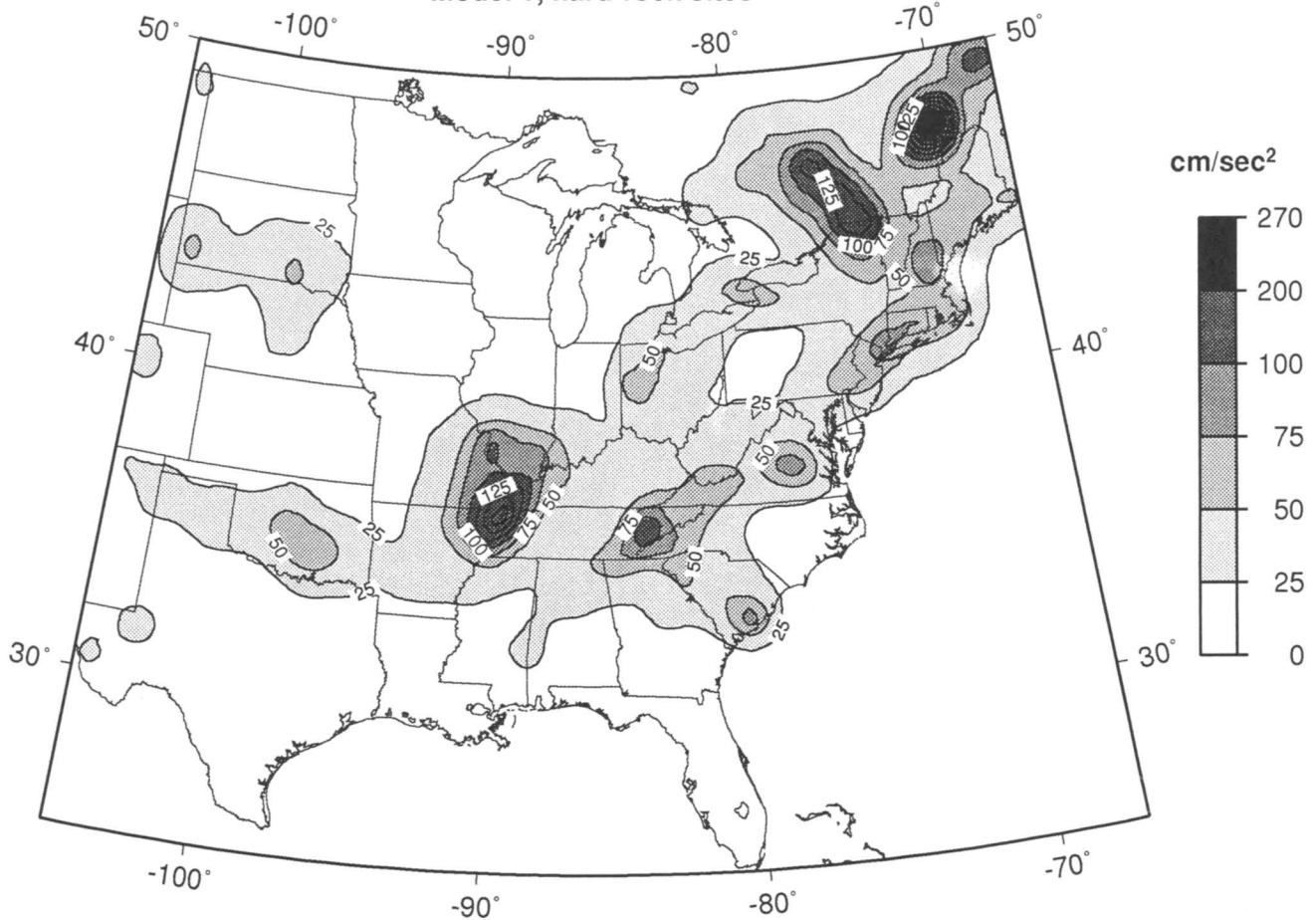
Now the annual rate $\lambda(u > u_0)$ of exceeding ground motion u_0 at a specific site is determined from a sum over distance and magnitude:

$$\lambda(u > u_0) = \sum_k \sum_l 10^{\log(N_k/T) - b(M_l - M_{ref})} P(u > u_0 | D_k, M_l) \quad (2)$$

where k is the index for the distance bin and l is the index for the magnitude bin. T is the time in years of the earthquake catalog used to determine N_k . The first factor in the summation is the annual rate of earthquakes in the distance bin k and magnitude bin l . The b -value is taken to be uniform throughout most of the area (see below). $P(u > u_0 | D_k, M_l)$ is the probability that u at the site will exceed u_0 , for an earthquake at distance D_k with magnitude M_l . This probability is dependent on the attenuation relation and the standard

Peak Accelerations with 10% Probability of Exceedance in 50 Years

Model 1; hard-rock sites



▲ **Figure 5** Trial ground-motion map derived from smoothed m_b 3 and larger earthquakes since 1924 (model 1), 10% probability of exceedance in 50 years. Hazard is calculated for earthquakes between m_b 4.5 and 7.0. Values are peak ground acceleration in cm/sec^2 for hard rock sites. Contour interval is 25 cm/sec^2 .

deviation (variability) of the ground motion for any specific distance and magnitude.

The hazard from model 3 is calculated using one large area source zone, where the a and b values are assumed to be uniform throughout the zone. The basic calculation is the same as equation (2), but the summation is taken over cells within the source zone. Now the values of N_k are uniform throughout the source zone and are determined from the area-normalized value of a found for the entire zone. In model 4 the hazard is calculated for individual faults, each with a specified magnitude and recurrence rate.

For all models, earthquake occurrence is assumed to be Poissonian, with time-independent probability. The annual probability of exceeding u_0 is essentially equal to the annual rate of exceedance $\lambda(u > u_0)$, for the annual probabilities of exceedance of interest here (0.0021 and less). After $l(u > u_0)$ is calculated for several values of u_0 , the ground motion with a certain probability of exceedance is determined by interpolation.

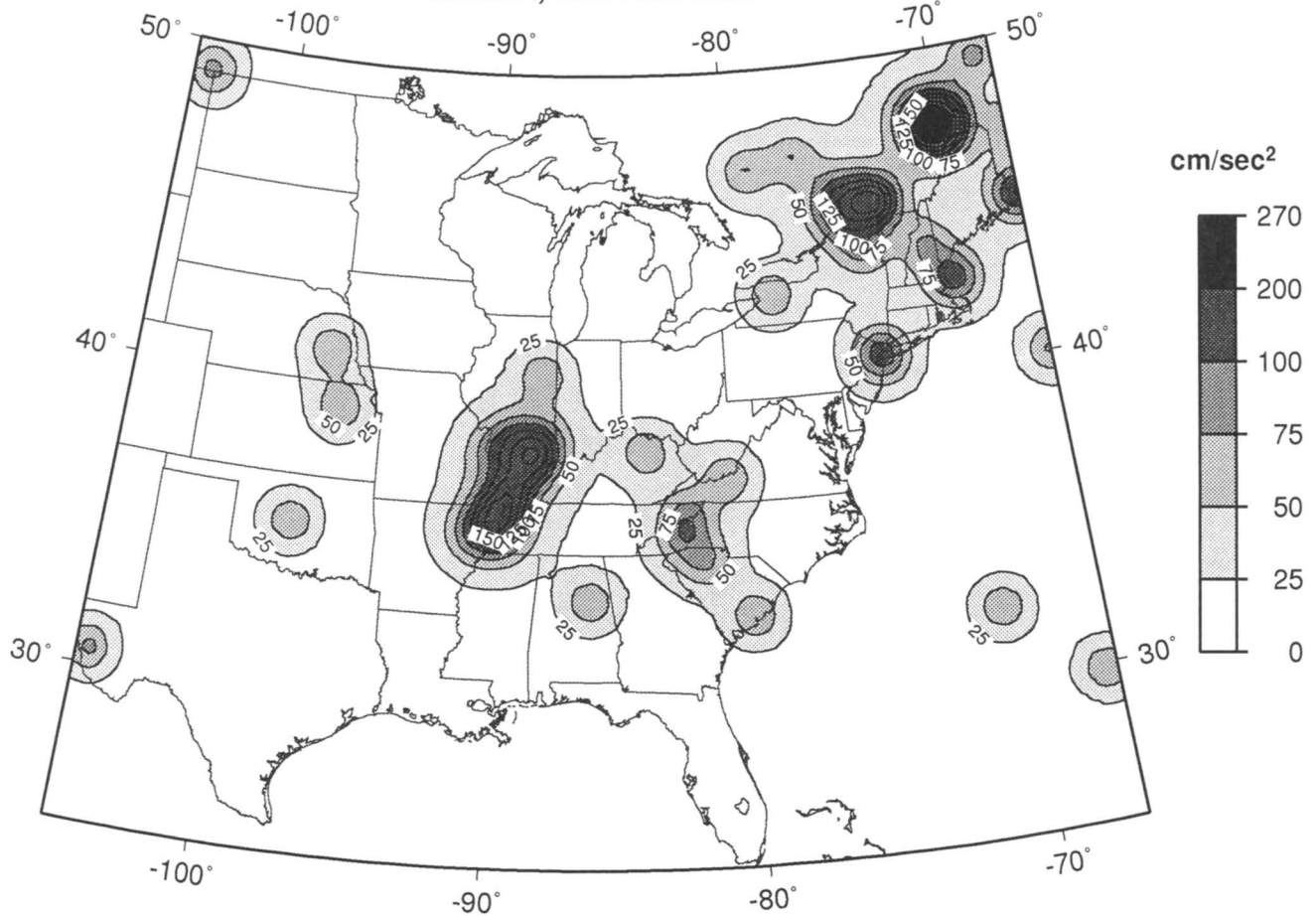
TRIAL MAPS

Figure 4 shows the smoothed values of 10^a from the m_b and larger earthquakes since 1924, using a correlation distance of 50 km. Larger correlation distances c were found to spread out the seismicity so that details were lost, whereas smaller values of c caused a very fragmented pattern emphasizing small clusters of magnitude 3 events. The 50 km correlation distance is also comparable to the location errors of the earlier earthquakes. Large values of 10^a in Figure 4 reflect areas of high concentrations of magnitude 3 and above events, such as New Madrid and Charlevoix (compare Figures 3a and 4).

Figure 5 is the trial map of the peak ground acceleration (PGA) with a 10% probability of exceedance in 50 years (return time of 475 years; annual probability of exceedance of 0.0021) derived from the grid of 10^a values in Figure 4. This map represents the probabilistic ground motions from model 1. The map is based on a grid of sites with a spacing of

Peak Accelerations with 10% Probability of Exceedance in 50 Years

Model 2; hard-rock sites



▲ **Figure 6** Trial ground-motion map derived from smoothed m_b 5 and larger earthquakes since 1700 (model 2), 10% probability of exceedance in 50 years. Hazard is calculated for earthquakes between m_b 4.5 and 7.0. Values are peak ground acceleration in cm/sec^2 for hard rock sites. Contour interval is $25 \text{ cm}/\text{sec}^2$.

about 40 km. The grid of $10''$ values had a spacing of about 11 km; using a grid spacing of about 5 km produced nearly identical results.

For all the ground-motion maps in this paper, I used the attenuation relation for hard rock sites in eastern North America published by Atkinson and Boore (1995). This relation was derived by stochastic simulations using propagation parameters determined from seismic network data and a source spectrum that, at high frequencies, corresponds to a stress drop of about 150 bars. I used the quadratic formula given in Atkinson and Boore (1995), which produces conservative values of ground motions for smaller events around magnitude 5. The “hard-rock” condition described by Atkinson and Boore (1985) presumes a shear wave velocity of 3.8 km/sec, which is much higher than the near-surface velocity of typical rock sites. To obtain values for typical rock sites, the values of ground motions in the maps should therefore be increased to account for the shear-wave velocity of the sites relative to 3.8 km/sec.

To obtain probabilistic ground motions for a stiff soil site

(shear-wave velocity 180–360 m/sec), the mapped values for hard rock sites should be multiplied by a factor of about 1.5 to 2.0 (see, e.g., Martin and Dobry, 1994).

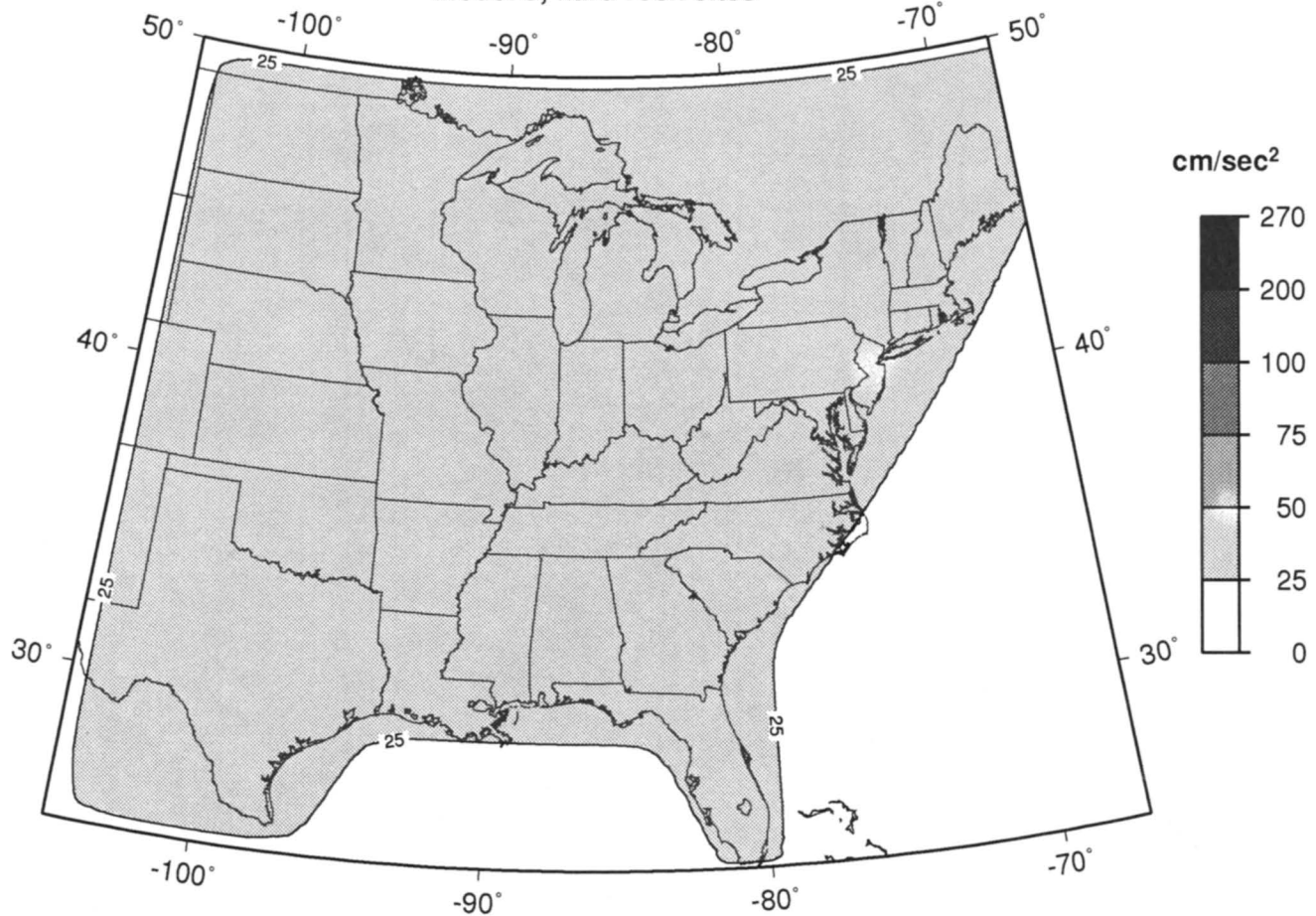
The Atkinson and Boore (1995) equations use moment magnitude, whereas the Seeber and Armbruster (1991) catalog gives a preferred magnitude for each event that is essentially m_b or m_{blg} . I convert their preferred magnitude to moment magnitude using the theoretical relation in Boore and Atkinson (1987). We are in the process of producing moment magnitude estimates for the events in the Seeber and Armbruster (1991) catalog by converting felt areas and maximum intensities directly to moment magnitude.

For this map and the others in this paper, I use a maximum M or m_b of 7.0 for the entire region. I found that varying the maximum magnitude between 6.0 and 7.0 made only a slight difference in the probabilistic value of PGA for this PE. Probabilistic ground motions at longer periods (e.g., ≥ 1 sec) and/or smaller PE values are sensitive to the maximum magnitude.

I used a regional b -value of 0.9 for the map, except for

Peak Accelerations with 10% Probability of Exceedance in 50 Years

Model 3; hard-rock sites



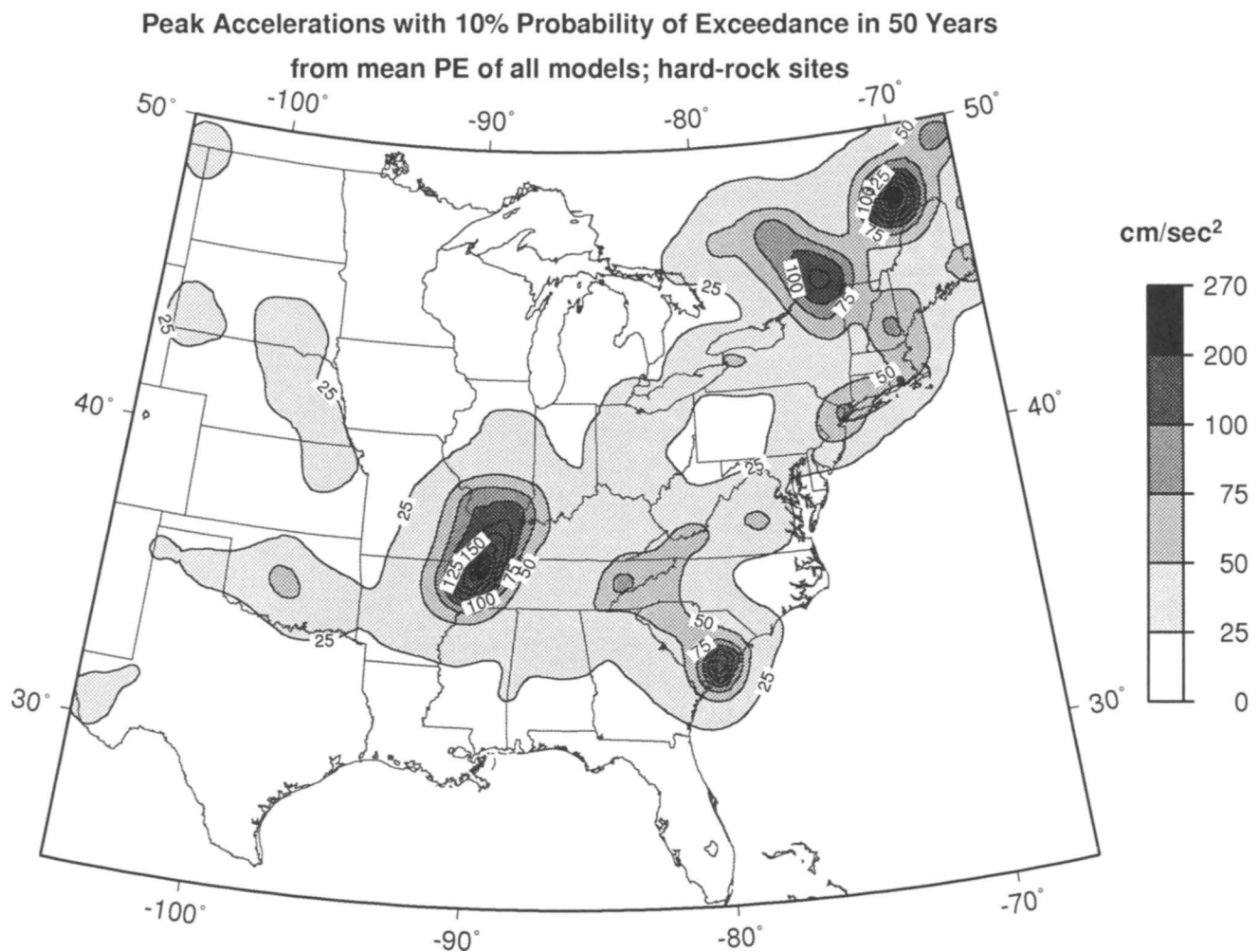
▲ **Figure 7** Trial ground-motion map from uniform background zone (model 3), 10% probability of exceedance in 50 years. Hazard is calculated for earthquakes between m_b 4.5 and 7.0. Values are peak ground acceleration in cm/sec^2 for hard rock sites.

the Charlevoix region. The value of 0.9 was determined from the number of m_b 5 and above earthquakes since 1924 compared to the number of m_b 3 and larger events in the same period (with aftershocks removed) in the entire region. Finding the slope defined by these two rates on the frequency-magnitude plot produces a b -value of 0.9. The Geological Survey of Canada has determined a b -value of 0.76 for the Charlevoix region (John Adams and Stephen Halchuk, pers. comm., 1994). I used this b -value for a 100 x 100 km zone encompassing the seismicity cluster near Charlevoix. I found that the probabilistic PGA (10% PE in 50 years) in Charlevoix increases by about a factor of 1.6 when the b -value is lowered from 0.9 to 0.76. The Charlevoix area was treated with a locally-specific b -value since it is unique in this region for producing several magnitude 6 main-shocks over the past 300 years.

The areas of large ground motions in Figure 5 simply indicate areas with larger numbers of magnitude 3 and larger events since 1924. The largest probabilistic ground motions are found for Charlevoix (about $270 \text{ cm}/\text{sec}^2$). The New

Madrid region shows ground motions of about $150 \text{ cm}/\text{sec}^2$, not counting the contribution from events larger than M 7.0. Other areas of relatively high ground motions are centered near Ottawa, along the coast of the U.S. between New Jersey and Massachusetts, and in the vicinity of eastern Tennessee, western North Carolina, and western Virginia. The areas around Charleston (South Carolina) and central Virginia also exhibit relatively high ground motions. Again, this map does not contain the hazard from events with magnitudes larger than 7.0, so it underestimates the probabilistic ground motions for New Madrid and Charleston. These events will be considered below.

Figure 6 displays a trial map for probabilistic ground motions derived from model 2, based on the m_b 5 and above earthquakes since 1700. I used a correlation distance of 75 km for the smoothing function. This is greater than that used for model 1, because of the larger location errors for the older events. This also helps to connect the ground motions for areas between m_b 5 events separated by up to about 200 km (e.g., events in eastern Nebraska and Kansas). This map



▲ **Figure 8** Trial probabilistic ground-motion map derived from four models (0.5, .25, .25, 1 weights, respectively). Values are peak ground acceleration in cm/sec^2 for hard rock sites. Contour interval is 25 cm/sec^2 .

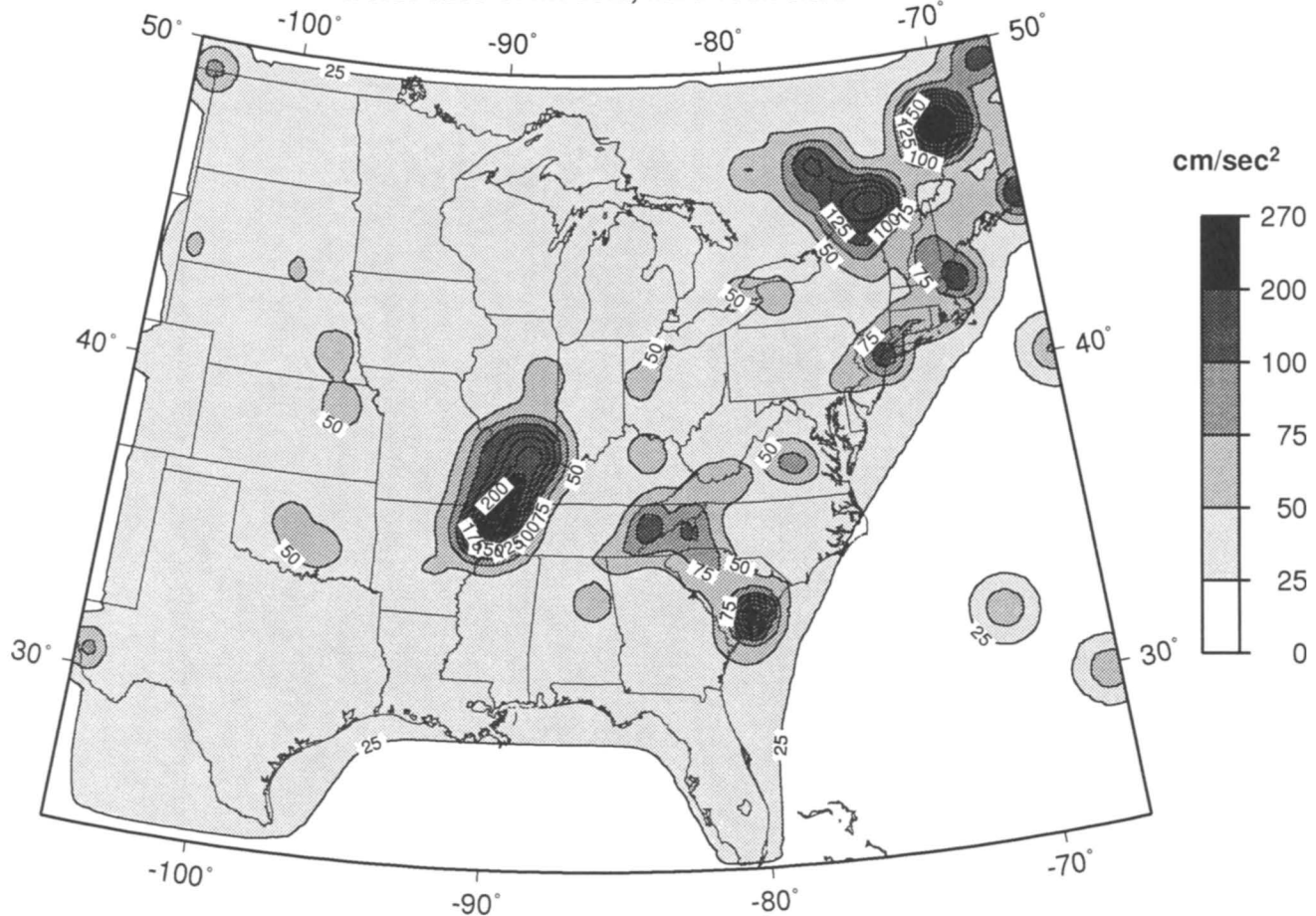
basically shows bulls-eyes where the M 5 and larger events have occurred. The values of ground motions are generally larger but more localized than those from model 1 (Figure 5). Note that the map in Figure 6 shows significant ground motions in eastern Nebraska and Kansas that are not present in the map made from M 3 events. This is the result of model 2 including the magnitude 5 events that occurred in that region in the 1800's.

A trial map of probabilistic ground motions for model 3 is shown in Figure 7. The 25 cm/sec^2 contour line basically follows the boundary of the source zone. The northern and southern borders of this zone are essentially arbitrary. I drew the northern boundary to include the seismicity in eastern Canada and to exclude the region of low seismicity in central Canada. The southern boundary corresponds roughly to the border of the U.S. The area within the 25 cm/sec^2 contour (Figure 7) has a probabilistic ground motion of about 30 cm/sec^2 (3% g), for 10% PE in 50 years.

I combined the maps from models 1–3, along with the hazard from moment magnitude 8.2 events in New Madrid

and moment magnitude 7.5 events in Charleston, to form a single probabilistic hazard map. For the New Madrid area, I used three parallel faults (similar to the geometry of Toro *et al.*, 1992) each separated by about 30 km to accommodate the uncertainty in the location of the faults which caused the 1811–12 earthquakes. I used a moment magnitude of 8.2 (see Johnston, 1992) and assumed a total recurrence rate of .001 per year for the three faults combined. This is consistent with recurrence estimates derived from paleoliquefaction evidence for the area (Schweig *et al.*, 1993). I also included the hazard for large earthquakes in the Charleston, South Carolina region. Here I used a moment magnitude of 7.5 (see Johnston, 1995) and a recurrence time of 600 years (Obermeier *et al.*, 1990). I assumed that the characteristic event occurred on a single fault corresponding to the location of the 1886 event. I did not consider the hazard from M > 7.0 earthquakes in the Wabash Valley, since the repeat time of these events is thought to be at least 4000 years (Obermeier *et al.*, 1992) and their hazard would not be significant for a map with a return time of 500 years. As with

Peak Accelerations with 10% Probability of Exceedance in 50 Years
 worst-case of models; hard-rock sites



▲ **Figure 9** Trial ground-motion map derived from worst-case of models (see text). Values are peak ground acceleration in cm/sec^2 for hard rock sites. Contour interval is 25 cm/sec^2 .

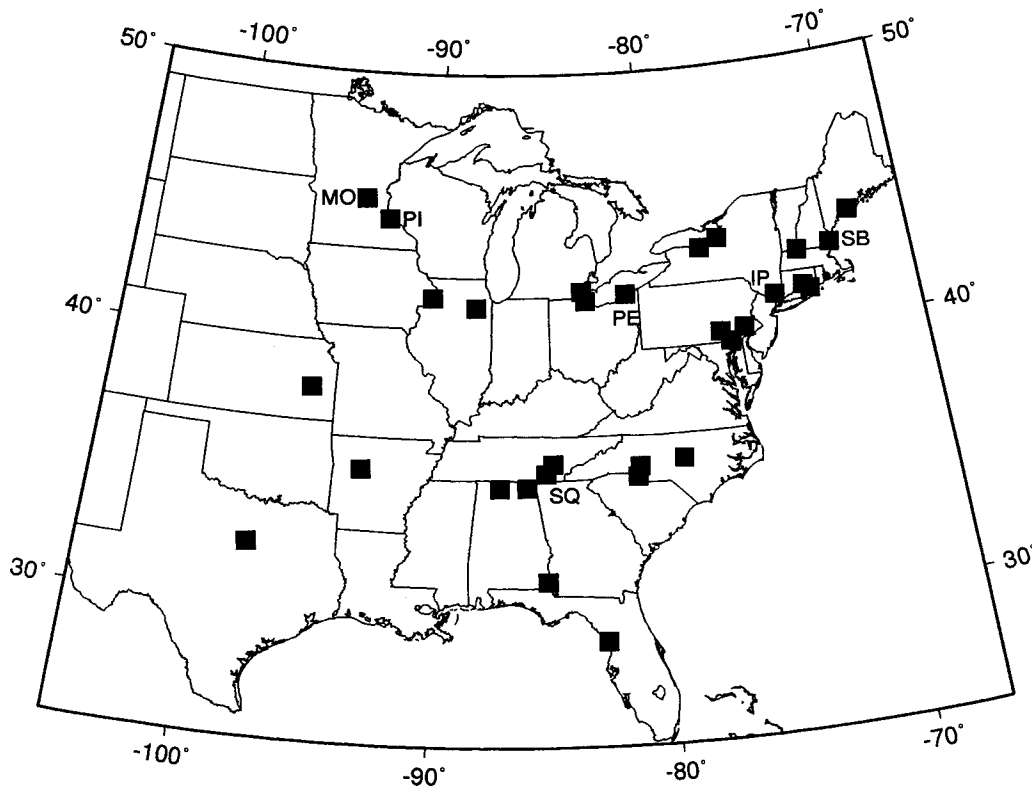
the other models, I assumed that the occurrence of large earthquakes was Poissonian (time-independent).

The combined probabilistic hazard map is shown in Figure 8. This map was derived from the weighted mean of the probabilities of exceedance from the four models at each location. Here I used weights of 0.5, 0.25, 0.25, and 1.0 for models 1, 2, 3, and 4 respectively. This map puts more weight on model 1 which was derived from the magnitude 3 and larger events. The weighting scheme is subjective; other schemes could be used. While this map combines all four models into one, there is a disadvantage. This map averages the hazard from the three models, which can result in areas with lower ground motions than that made from model 3 alone. Thus, this map would underestimate the probabilistic ground motions compared to those predicted just by extrapolating the rates of magnitude 3 and larger earthquakes. Of course, this is compensated for by raising the ground motions somewhat in areas that haven't had any historical seismicity. This map essentially has a floor of about 1.5% g in areas that have not had $m_b 3$ or larger earthquakes since 1924

or $m_b 5$ and larger earthquakes since 1700 (in the historic record). This floor is a result of the contribution from model 3 (uniform background zone), with a 0.25 weight.

An important issue in hazard mapping is whether it is desirable to make such a combined probabilistic map as Figure 8 which lowers the hazard estimates in the areas of higher hazard in order to raise the hazard values in areas with low hazard. This dilemma is also discussed in Adams *et al.*, (1995), for hazard maps for Canada.

Another approach is to make a map which shows the highest value of the probabilistic ground motions from the models, for each location on the map. First, I added the probability of exceedance from model 4 ($M 7.0$ and larger events) to each of models 1–3. This was done so that models 1–3 will each contain the hazard from $M 7.0$ and larger earthquakes. Then, for each site I found the largest probabilities of exceedance between the three models. This was used to calculate the ground motions for that location. The “worst-case” map is shown in Figure 9. It is not a probabilistic hazard map in the sense that it does not preserve the historical rate



▲ **Figure 10** Map showing reactor sites used in comparison of four-model and EPRI methods. Labeled sites are discussed in text: SB (Seabrook), SQ (Sequoyah), IP (Indian Point), PE (Perry), MO (Monticello), and PI (Prairie Island).

of moderate earthquakes. Now, the ground motions from model 3 comprise a floor with a value of 3% g, larger than in the probabilistic map in Figure 8. The worst-case map highlights more strongly than the probabilistic map the places which have experienced magnitude 5 and greater earthquakes in the past.

The worst-case map does not reduce the hazard calculated from extrapolating the rates of magnitude 3 and larger events (model 1), unlike the probabilistic map. One can argue that, in light of uncertainties in the cause of seismicity in the central and eastern U.S., it is reasonable to use a hazard map with the highest value of the four models. Adams *et al.* (1995) makes such an argument to use the worst case of their two models based on historical seismicity and regional geologic structures, for their seismic hazard maps of Canada.

COMPARISON WITH EPRI STUDY

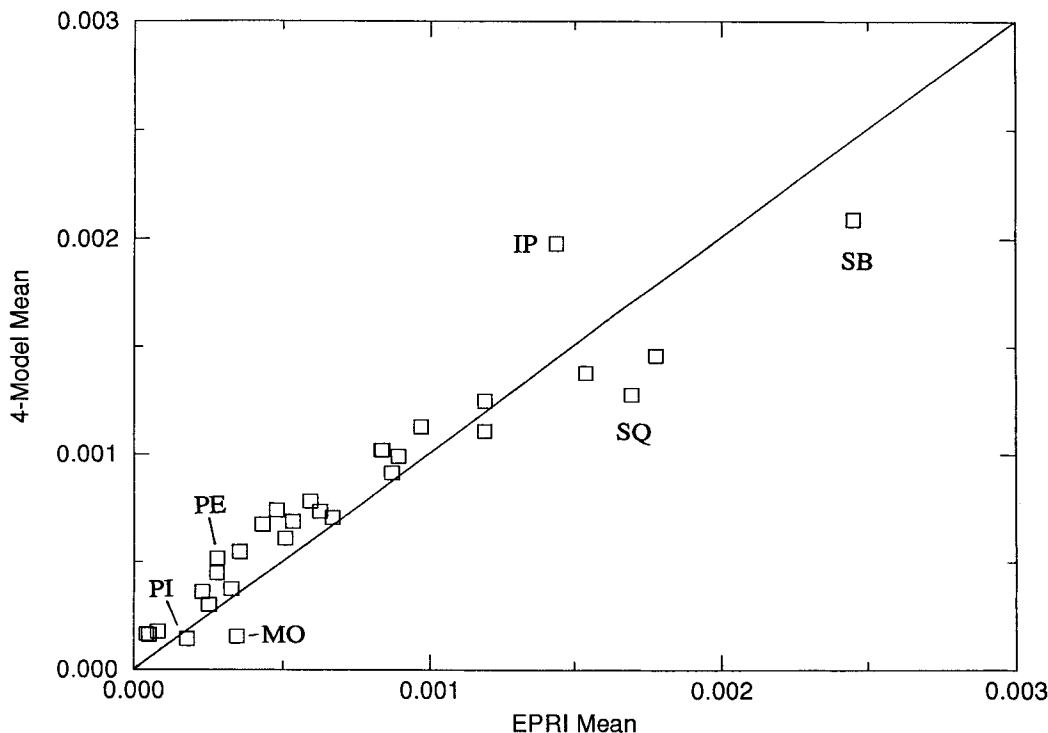
I compared the results of the four-model method to those from the EPRI study for 30 nuclear power plant sites. I chose all of the sites classified as rock sites by EPRI. These sites are shown in Figure 10. I used the same attenuation relations as the EPRI study: McGuire *et al.* (1988) with weight 0.5, Boore and Atkinson (1987) with weight 0.25, and Nuttli (1986) with weight 0.25. The same variability of ground motion was applied for the two methods. I have not yet done a comparison with the LLNL study because it uses a much more complex set of weighted ground motion relations. I used a

minimum m_b of 5.0 and maximum m_b of 6.5, the former identical to that used by EPRI and the latter a representative average of those assigned by the EPRI teams for most regions. I used a regional b -value of 0.9, based on the seismicity of the entire region (see above). For sites within 500 km of New Madrid, I added the hazard from M 8.2 earthquakes as described above. For sites within 500 km of Charleston, I added the hazard from M 7.5 earthquakes with a repeat time of 600 years. As before, I used the weighting scheme of 0.5, 0.25, 0.25, 1.0 for models 1, 2, 3, and 4, respectively.

Figure 11 shows the comparison between the mean values of probability of exceeding 5% g obtained from the four-model method and the EPRI study. The diagonal line in the plot represents perfect agreement between the two methods. The four-model and EPRI probabilities agree to within a factor of four for all 30 sites. For all but four sites, the methods agree to within a factor of 1.6. The four sites with discrepancies between a factor of 1.6 and 3.7 had very low hazard. I consider the agreement between the two methods to be quite good, considering that the difference between the 15th and 85th percentiles found by EPRI generally ranges between a factor of eight to about twenty (depending on the site), for PE's of this ground motion level.

For most sites, the four-model method produces probabilities somewhat higher than the EPRI study. The most extreme exception is the Monticello site in Minnesota (see Figure 10), where the four-model probability is 0.44 times that of the EPRI study. The four-model method assigns

Annual Probability of Exceeding 5%g



▲ **Figure 11** Comparison of probability of exceeding 5% g between four-model method and EPRI. Mean probabilities are used for both studies. Solid line represents perfect agreement between the two methods. Note the good agreement between the probabilities derived from these methods. See caption for Figure 10 for site labels.

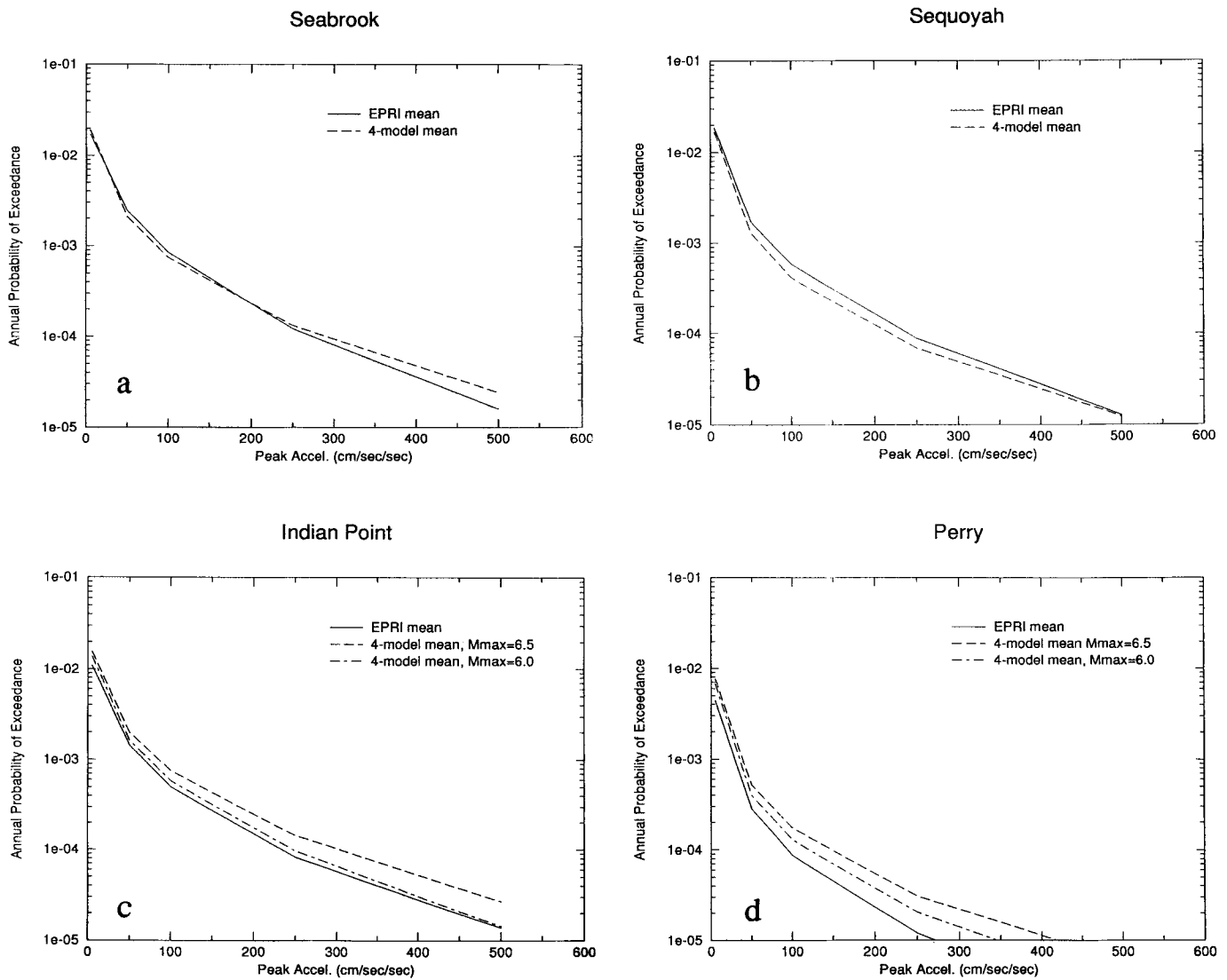
similar probabilities to Monticello and Prairie Island, which is about 100 km to the southeast. The EPRI study gives a probability at Monticello about twice that of Prairie Island. This is probably caused by the decision of three of the six EPRI teams to draw a source zone in western Minnesota that encompasses some m_b 3–4 historic earthquakes in western Minnesota (see Figure 1). This source zone follows the Great-Lakes Tectonic Zone-Colorado Lineament (EPRI, 1986), which has been identified as a pre-Cambrian suture zone. It is notable that none of the 13 experts involved in a similar study conducted by Lawrence Livermore National Lab (LLNL) chose to make a source zone based on this feature (Bernreuter *et al.*, 1989). The LLNL probabilities for Monticello and Prairie Island are about equal to each other.

For the 30 sites, the four-model approach gives mean values comparable to the EPRI study, without the involved process of expert elicitation. This is probably the result of the EPRI experts either basing their source zones on the historic seismicity or using locally-determined seismicity parameters. Most EPRI experts partly used seismicity parameters (a and b-values) that were determined in cells one degree in latitude by one degree in longitude. This local determination of a-values is similar in philosophy to the procedure used in model 1 (T. F. O'Hara, pers. comm.). Of course the expert elicitation allows for the quantification of the uncertainties of seismicity parameters based on the range of expert opinions. However, the four-model method can also be used to quan-

tify uncertainties in seismicity parameters based on models 1–3 which span a range of possible hazard models.

Hazard curves derived from the four-model method and the EPRI method are in reasonable agreement. Figure 12 displays the hazard curves for Seabrook (New Hampshire), Sequoyah (eastern Tennessee), and Indian Point (New York), and Perry (Ohio). For Seabrook and Sequoyah, there is good agreement between the mean curves for the four-model and EPRI methods, even down to annual probability levels of 2×10^{-5} . For example, the ground motions at Sequoyah for an annual PE of 1×10^{-3} derived from the four-model method are 87% of the EPRI value. For Seabrook the ground motions from the four-model method for that PE are 93% of the EPRI value.

For Indian Point and Perry, the hazard curves from the four-model method are somewhat higher than those from the EPRI study. At 1×10^{-3} PE, the ground motions from the four-model method at Indian Point and Perry are 125% and 130%, respectively, of those found by the EPRI study. For these sites, the ratio between the four-model and EPRI PE's increases as the probability level decreases. At Perry, the PE for 250 cm/sec^2 derived by the four-model method is about 2.5 times that of the EPRI result. The discrepancy is probably caused by: 1) the relatively large weighting of magnitude 3 seismicity in the four-model method and 2) differences in maximum magnitude between the four-model and EPRI studies. The plots for Indian Point and Perry also show the



▲ **Figure 12** Hazard curves derived by the four-model ($M_{max} = 6.5$) and EPRI methods for a) Seabrook, b) Sequoyah, c) Indian Point, and d) Perry. Note the good agreement between the two methods for probability levels down to 1×10^{-4} (and lower for Seabrook and Sequoyah). For Indian Point and Perry, hazard curves are also shown for the four-model method using a M_{max} of 6.0.

hazard curves derived from the four-model method using a maximum magnitude of 6.0, rather than 6.5 (see Figure 12). This decrease in M_{max} has a large effect on the probability levels at large ground motions and can account for some of the difference between the four-model and EPRI values at low probability levels. Generally speaking, experts in the EPRI study picked M_{max} values between 5.5 and 7.0, for most areas of the central and eastern U.S.

It is notable that there was a m_b 4.9 earthquake near the Perry site in 1986. This event occurred after the period of the catalog used in the four-model calculations. The hazard at this site derived by the four-model method is larger than that from the EPRI study. The occurrence of the Perry earthquake provides further justification for using the previous occurrence of magnitude 3 events to assess hazard (*i.e.*, model 1),

as this area of Ohio had several M3 events between 1924 and 1984 (see Figure 3a).

CONCLUSIONS

I have presented a simple four-model method which produces probabilistic hazard maps largely without the use of seismic source zones. This method uses spatially-smoothed representations of historic seismicity to directly calculate probabilistic hazard.

Many of the participants of the northeast workshop felt that source zones based on geologic criteria should become more important when assessing hazard for low probabilities of exceedance (less than 0.001/year). This reflects a concern that the historical seismicity may not be a good indicator of

future seismicity over a long period of time. However, the good agreement with the EPRI hazard curves down to PE of 1×10^{-4} indicates that the four-model method can be reasonably applied even for these low probability levels. Of course, maps with 10% PE in 250 years will be more speculative than those with shorter return times.

I welcome comments, suggestions, and criticisms of the methodology presented here. The next step is to collect the latest research bearing on the locations and recurrence times of large earthquakes ($M > 7.0$) in the central and eastern U.S. This will be done at the regional workshop for the central and southeastern U.S. to be held in April 1995 (after this paper was written). Taking this input, we will then produce interim hazard maps for PGA and spectral response at various periods. The interim maps will be distributed to workshop participants and others for their review. We also plan to do a formal error analysis for selected sites, incorporating uncertainties in ground motion attenuation, hazard models, maximum magnitude, and seismicity parameters. ☒

**U.S. Geological Survey
MS 966, Box 25046
Denver Federal Center
Denver, CO 80225
(A. F.)**

ACKNOWLEDGMENTS

I thank David Perkins and Charles Mueller for their helpful reviews. An anonymous reviewer provided useful comments which led to the improvement of the paper. Margaret Hopper removed the aftershocks from the catalog. Tom O'Hara kindly provided the EPRI results, helpful advice, and comments on the paper. Rus Wheeler, Tom Hanks, John Adams, Joan Gomberg, Steve Horton, Noel Barstow, and Klaus Jacob provided helpful comments on the paper. David Perkins described his work on using historic seismicity to calculate hazard. Paul Pomeroy, Tom Hanks, Tom O'Hara, and Klaus Jacob, among others, suggested the comparison between the four-model and EPRI results. Paul Thenhaus, Rus Wheeler, and John Adams provided useful discussions about source zones in the region. I thank all the participants of the northeast workshop for their valuable suggestions and feedback.

REFERENCES

Adams, J., P. W. Basham, and S. Halchuk (1995). Northeastern North American earthquake potential—new challenges for seismic hazard mapping, in Current Research 1995-D, Geological Survey of Canada, pp. 91–99.

Algermissen, S. T. and D. M. Perkins (1976). A probabilistic estimate of maximum acceleration in rock in the contiguous United States, U.S. Geological Survey open file report 76-416.

Algermissen, S. T., D. M. Perkins, P.C. Thenhaus, S.L. Hanson, and B.L. Bender, (1990). Probabilistic Earthquake Acceleration and Velocity Maps for the United States and Puerto Rico, U.S. Geological Survey, Miscellaneous Field Studies Map MF-2120.

Atkinson, G. M. and D.M. Boore (1995). Ground motion relations for eastern North America, *Bull. Seism. Soc. Am.* **85**, 17–30.

Bender, B. (1983). Maximum likelihood estimation of b values for magnitude grouped data, *Bull. Seism. Soc. Am.* **73**, 831–851.

Bernreuter, D. L., J. B. Savy, R. W. Mensing, and J. C. Chen (1989). Seismic hazard characterization of 69 nuclear power plant sites east of the Rocky Mountains, U.S. Nuclear Regulatory Commission, technical report NUREG/CR-5250 UCID-21517, prepared by Lawrence Livermore National Laboratory.

Boore, D. M. and G. M. Atkinson (1987). Stochastic prediction of ground motion and spectral response parameters at hard-rock sites in eastern North America, *Bull. Seism. Soc. Am.* **77**, 440–467.

Cornell, C. A. (1968). Engineering seismic risk analysis, *Bull. Seism. Soc. Am.* **58**, 1583–1606.

Electric Power Research Institute (1986). Seismic hazard methodology for the central and eastern United States, 10 volumes., *EPRI report NP-4726*, Electric Power Research Institute, Palo Alto.

Herrmann, R. B. (1977). Recurrence relations, *Earthquake Notes* **48**, 47–49.

Jacob, K., J. Armbruster, N. Barstow, and S. Horton (1994). Probabilistic ground motion estimates for New York: comparison with design ground motions in national and local codes, in *Proceedings of fifth U.S. National Conference on Earthquake Engineering*, Chicago, v. III, 119–128.

Johnston, A. C. (1992). The stable continental region earthquake data base, in Methods for assessing maximum earthquakes in eastern United States, K. J. Coppersmith, A. C. Johnston, L. R. Kanter, R. R. Youngs, A. G. Metzger (Editors), *EPRI Report RP-2556-12*, Electric Power Research Institute, Palo Alto.

Johnston, A. C. (1995). Moment magnitude assessment of stable continental earthquakes, Part 2: historical seismicity, submitted to *Geophysical Journal International*.

Martin, G. R. and R. Dobry (1994). Earthquake site response and seismic code provisions, *NCEER Bulletin* **8**, 1–6.

McGuire, R. K, G. R. Toro, and W. J. Silva (1988). Engineering model of earthquake ground motion for eastern North America, *EPRI report NP-6074*, Electric Power Research Institute.

Nuttli, O. W. (1986). Letter to J. B. Savy, reproduced in Bernreuter *et al.* (1989).

Obermeier, S. F., R. B. Jacobson, J. P. Smoote, R. E. Weems, G. S. Gohn, J. E. Monroe, and D. S. Powers (1990). Earthquake-induced liquefaction features in the coastal setting of South Carolina and in the fluvial setting of the New Madrid seismic zone, *U.S. Geol. Survey, Prof. Paper* 1504, 44 pp.

Obermeier, S. F., P. J. Munson, C. A. Munson, J. R. Martin, A. D. Frankel, T. L. Youd, and E. C. Pond (1992). Liquefaction evidence for strong Holocene earthquake(s) in the Wabash Valley of Indiana-Illinois, *Seis. Res. Lett.* **63**, 321–336.

Schweig, E. S., M. Tuttle, Y. Li, J. Craven, M. Ellis, M. Guccione, R. Lafferty, and R. Cande (1993). Evidence for recurrent strong earthquake shaking in the past 5,000 years, New Madrid region, central U.S., abstract, *EOS (Trans. Am. Geophys. U.)* **74**, 438.

Seeber, L. and Armbruster, J. G. (1991). The NCEER-91 earthquake catalog: improved intensity-based magnitudes and recurrence relations for U.S. earthquakes east of New Madrid, National Center for Earthquake Engineering Research, NCEER-91-0021.

Sibol, M. S., Bollinger, G. A., and J. B. Birch (1987). Estimation of magnitudes in central and eastern North America using intensity and felt area, *Bull. Seism. Soc. Am.* **77**, 1635–1654.

Toro, G. R., W. J. Silva, R. K. McGuire, and R. B. Herrmann (1992). Probabilistic seismic hazard mapping of the Mississippi embayment, *Seism. Res. Lett.* **63**, 449–476.

Veneziano, D. and Pais, A. L. (1986). "Automatic source identification based on historical seismicity," Proceedings, 8th European conference on Earthquake Engineering, Lisbon, Portugal.

Weichert, D. H. (1980). Estimation of earthquake recurrence parameters for unequal observation periods for different magnitudes, *Bull. Seism. Soc. Am.* **70**, 1337–1356.